




Inhibition of nitrate reduction by NaCl adsorption on a nano-zero-valent iron surface during a concentrate treatment for water reuse

Yuhoon Hwang, Dogun Kim & Hang-Sik Shin


To cite this article: Yuhoon Hwang, Dogun Kim & Hang-Sik Shin (2015) Inhibition of nitrate reduction by NaCl adsorption on a nano-zero-valent iron surface during a concentrate treatment for water reuse, Environmental Technology, 36:9, 1178-1187, DOI: [10.1080/09593330.2014.982723](https://doi.org/10.1080/09593330.2014.982723)


To link to this article: <http://dx.doi.org/10.1080/09593330.2014.982723>

 View supplementary material [↗](#)

 Accepted author version posted online: 31 Oct 2014.
Published online: 02 Dec 2014.

 Submit your article to this journal [↗](#)

 Article views: 92

 View related articles [↗](#)

 View Crossmark data [↗](#)

 Citing articles: 2 View citing articles [↗](#)

Inhibition of nitrate reduction by NaCl adsorption on a nano-zero-valent iron surface during a concentrate treatment for water reuse

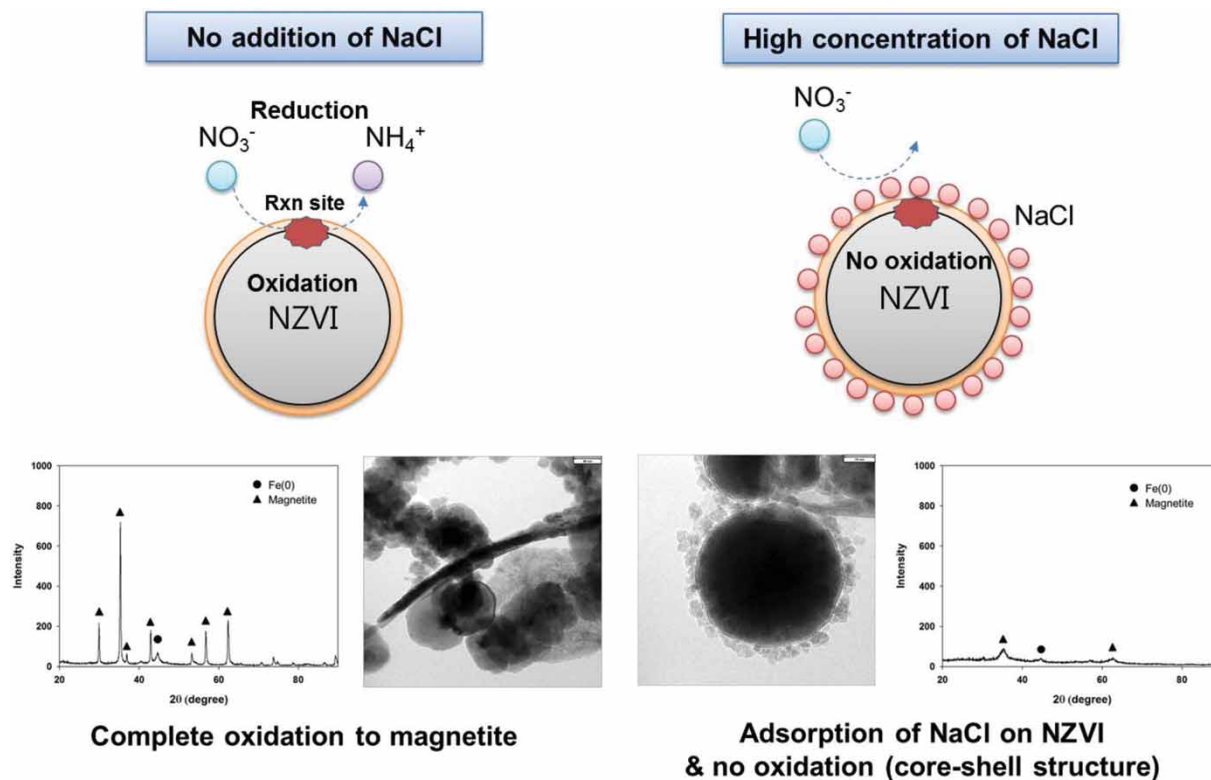
Yuhoon Hwang^{a,c*}, Dogun Kim^b and Hang-Sik Shin^c

^aDepartment of Environmental Engineering, Technical University of Denmark, Miljøvej, Building 113, Lyngby 2800, Denmark;

^bDepartment of Civil Engineering, Kyunghee University Global Campus, 1732 Deogyong-daero, Giheung-gu, Yongin-si, Gyeonggi-do 446-701, Republic of Korea; ^cDepartment of Civil and Environmental Engineering, Korea Advanced Institute of Science and Technology, 291 Daehak-ro, Yuseong-gu, Daejeon 305-701, Republic of Korea

(Received 19 May 2014; accepted 21 August 2014)

Nanoscale zero-valent iron (NZVI) has been considered as a possible material to treat water and wastewater. However, it is necessary to verify the effect of the matrix components in different types of target water. In this study, different effects depending on the sodium chloride (NaCl) concentration on reductions of nitrates and on the characteristics of NZVI were investigated. Although NaCl is known as a promoter of iron corrosion, a high concentration of NaCl (> 3 g/L) has a significant inhibition effect on the degree of NZVI reactivity towards nitrate. The experimental results were interpreted by a Langmuir–Hinshelwood–Hougen–Watson reaction in terms of inhibition, and the decreased NZVI reactivity could be explained by the increase in the inhibition constant. As a result of a chloride concentration analysis, it was verified that 7.7–26.5% of chloride was adsorbed onto the surface of NZVI. Moreover, the change of the iron corrosion product under different NaCl concentrations was investigated by a surface analysis of spent NZVI. Magnetite was the main product, with a low NaCl concentration (0.5 g/L), whereas amorphous iron hydroxide was observed at a high concentration (12 g/L). Though the surface was changed to permeable iron hydroxide, the Fe(0) in the core was not completely oxidized. Therefore, the inhibition effect of NaCl could be explained as the competitive adsorption of chloride and nitrate.



Keywords: nano zero-valent iron; nitrate reduction; reverse osmosis concentrate; NaCl adsorption; inhibition

*Corresponding author. Email: yuoh@env.dtu.dk

1. Introduction

The application of zero-valent iron (ZVI) has emerged as one of the most effective technologies for water treatment and soil/groundwater remediation processes.[1] Due to its suitable redox potentials, it has been used for the removal of a wide variety of pollutants, including chlorinated hydrocarbons, nitrobenzenes, chlorinated phenols, polychlorinated biphenyls, heavy metals, and anions.[2] With its small size and high specific surface area, nanoscale zero-valent iron (NZVI) is a promising and flexible technology for the *in situ* remediation of groundwater contaminants that are amenable to reduction by ZVI.[3]

Despite the great potential of NZVI, scant attention has been paid to the effects of the composition of water on the reactivity of NZVI, despite the fact that it is important to evaluate these factors to determine the potential use of NZVI in practical applications. Recently, several papers reported the application of NZVI to actual wastewater and its reactivity. Klimkova et al. [4] and Crane et al. [5] reported an experiment which involved the application of NZVI to acid mine water. These two cases clearly show that the reaction mechanisms and reactivity levels in real wastewater treatment applications can differ significantly in synthetic contaminant solutions due to the complex chemical compositions of environmental water samples. Due to the significant inhibition effect of real water samples, research approaches have focused not on process performance levels but on reaction and inhibition mechanisms.

In this study, the concentrate generated from a water reuse process was chosen as the target water sample for the application of NZVI. The reverse osmosis (RO) process is generally applied as a desalting process in water reuse. This technology employs semi-permeable membranes that allow for the separation of a solution into two streams: the permeate stream, which contains purified water that passes through the membrane, and the concentrate stream, which is the portion that contains salts and the retained compounds. Therefore, it is necessary to determine suitable and environmentally friendly management options for the concentrate stream.[6]

Typically, RO concentrate generated in municipal membrane desalination sites has been disposed of as surface water or sent to wastewater treatment plants, to the subsurface, or to an evaporation pond.[7] The discharge of concentrate to another water body can cause environmental pollution due to the high concentrations of pollutants and salt. While concentrate from a water reuse plant shows much less salinity, it has a higher pollutant load compared with the case of seawater desalination. Due to the adverse effects of brine disposal, together with its associated costs, current research is focused on reducing the impact of concentrates by diminishing their pollutant loads. Most reported studies have focused on reducing global parameters related to organic contamination (e.g. the chemical oxygen demand, total organic carbon)

by coagulation, adsorption, or by advanced oxidation processes.[8–12]

RO concentrate contains high concentrations of ionic matter (salt), which is retained by a semi-permeable RO membrane. The high concentration of salt existing in RO concentrate can affect the NZVI characteristics and reactivity; therefore, the impact of a high concentration of salt on the NZVI characteristics needs to be verified prior to its application. Several studies have reported the effects of ionic matter on the reactivity levels and characteristics of NZVI. Most papers reported that the ZVI reactivity increased by as much as 40 times with 0.5–50 mM of a sodium chloride (NaCl) solution.[13–15] Because the Cl^- increases the permeability of the oxide film on the ZVI surface, zero-valent iron is not readily passivated in the solution in a process known as pitting corrosion. However, the concentration of ionic matter in the RO concentrate in this study can be much higher (≈ 20 g/L; 341.9 mM) than those in previous studies. Therefore, research on the effect of a high salt concentration on NZVI reactivity should be undertaken in an effort to understand the feasibility of NZVI for real applications to high-saline water such as RO concentrate.

In this study, the effect of ionic matter on the degree of NZVI reactivity was evaluated using a nitrate reduction batch test, which serves as an indicator for quantifying the reducing power of NZVI. Sodium chloride (NaCl) was selected as the model ionic matter in the batch test. The experimental results were interpreted by a Langmuir–Hinshelwood–Hougen–Watson (LHHW) reaction with inhibition. Fresh and spent NZVI are characterized, and the changes in the NZVI characteristics are discussed with the results of a kinetic study.

2. Methods

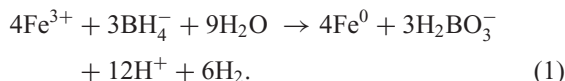
2.1. Chemicals

Ferric chloride (Junsei Chemical Co., Japan) and sodium borohydride (Samchun Pure Chemical Co., Korea) were used for the synthesis of NZVI. To prepare a reactant stock solution, potassium nitrate (Duksan Pure Chemical Co., Korea) was used, while sodium hydroxide and hydrochloric acid (Jin Chemical Pharmaceutical Co., Korea) were used to adjust the pH. Sodium chloride (Samchun Pure Chemical Co., Korea) was used as the model ionic matter. All solutions were prepared using deionized water after deoxygenation by purging with argon gas for 3 h.

2.2. NZVI synthesis

In this study, the mild chemical reduction of metal salts in the solution phase was used to prepare the NZVI.[3] The synthesis of the NZVI was conducted in a 500-mL four-open-neck flask reactor. One of the necks had a tunable mechanical stirrer installed and running at 60–500 rpm (MS3060, Mtops, Korea). The stirring speed was adjusted

to 200 rpm for the NZVI synthesis step and to 60 rpm for aging. A sodium borohydride solution at an amount of 250 mL (358.4 mM) was introduced into 250 mL of a ferric ion (Fe^{3+}) solution (71.7 mM) using a peristaltic pump (10 mL/min) to reduce the ferric ion to NZVI. The reduction reaction is as follows:



The NZVI was collected by the vacuum filtration of the solution after an ageing period of 20 min. The collected particles were then washed three times with ethanol and dried in an anaerobic chamber ($\text{N}_2:\text{H}_2 = 95:5$). For the batch nitrate reduction test, the prepared NZVI was washed with deoxygenated deionized water and introduced immediately into a nitrate solution.

2.3. Site description and RO concentrate characteristics

The RO concentrate characteristics were obtained from a wastewater reclamation pilot plant located at the 'Y' WWTP in Korea. The reclamation process was ultrafiltration followed by RO. The total capacity of the pilot plant was 96 m³/day. The measured Na^+ and Cl^- concentrations were 1975 and 6176 mg/L, respectively. The Cl^- concentration appears to be higher than the theoretical composition of sodium chloride due to the presence of other cations, for example, Ca^{2+} or Mg^{2+} . The total dissolved solid concentration (TDS) of the RO concentrate was about 11.7 g/L, while TDS of the WWTP effluent was 3.0 g/L. To verify the effect of the TDS concentration on the NZVI reactivity and related characteristics, sodium chloride was selected as the model electrolyte. The range of the sodium chloride concentration was adjusted to 0–20 g/L. The TDS range was divided into low concentration (0–3 g/L) and high concentration (3–20 g/L) sections based on the TDS concentration of the WWTP effluent (3 g/L).

2.4. Evaluation of NZVI reactivity – batch test and reaction kinetics

Batch tests for nitrate reduction were conducted in 1 L Schlenk flasks. The reactor was filled with 750 mL of reactant solution containing nitrate, and the solution was purged with argon gas before the injection of NZVI. Then, 50 mL of a NZVI slurry containing 1 g of NZVI was added to the reactor. The final concentrations of nitrate and NZVI were 100 mg NO_3^- -N/L (7.1 mM) and 1250 mg Fe/L (22.4 mM), respectively. The solution was continuously stirred with a mechanical stirrer and samples were taken periodically. The stirring speed was adjusted to 200 rpm during the batch test for vigorous mixing. The high mixing intensity was applied to minimize the limits of mass

transfer and to secure sufficient contact efficiency between the nitrate and the NZVI, according to Choe et al.[16] The samples were filtered with 0.45 μm syringe filters and analysed immediately. An anoxic condition was maintained by the continuous blowing of argon gas (500 mL/min) into the reactor.

A pseudo-first-order kinetic equation has been widely used for the interpretation of nitrate reduction results by NZVI.[17] However, the adsorption of nitrate on the NZVI surface and the pH change during the reaction should be considered in cases of nitrate reduction by NZVI. A lack of consideration of the adsorption and desorption can lead to the overestimation of ammonia generation as the reaction product of the nitrate reduction.[18] Therefore, the LHHW reaction was proposed for the interpretation of the nitrate reduction. The LHHW equation is used for heterogeneous surface catalysis, during which the reaction occurs between species that are adsorbed on a surface.[19] It is assumed that two molecules are adsorbed on adjacent sites and that a reaction takes place via an activated complex on the surface to yield the reaction products.

Moreover, inhibition was inevitable due to the formation of a passivation layer on the NZVI surface; this can be affected by the NZVI characteristics (e.g. the size and surface area).[20–22] Therefore, it is necessary to consider the inhibition of NZVI during the nitrate reduction process.

The reaction rate of the nitrate reduction was interpreted by the following kinetic formulation with the first-order inhibition of NZVI:

$$\frac{dC}{dt} = -C_{\text{cat}} \frac{kC_{\text{NO}_3}}{1 + KC_{\text{NO}_3}} \times e^{(-b_N \times (C_{\text{NO}_3,0} - C_{\text{NO}_3,t}) / C_{\text{cat}})}. \quad (2)$$

Here, C_{NO_3} is the nitrate concentration (mg/L), C_{cat} is the NZVI dosage (mg/L), k is the reaction rate constant ($1/\text{g}_{\text{cat}}\text{min}$), K is the adsorption coefficient (L/mg), and b_N is the inhibition constant ($1/\text{min}$). The kinetic constants were obtained by curve fitting using Matlab R2012a (MathWorks, Inc. Massachusetts, USA)

2.5. Analytical items and methods

2.5.1. Nitrogen species (nitrate, nitrite, and ammonium) and TDS concentration

The nitrate, nitrite concentrations were analysed by ion chromatography (DX-120, Dionex Co., Sunnyvale, CA, USA) with an IonPac AS4A-SC carbonate eluent anion-exchange column. Ammonium and total nitrogen were analysed using a titrimetric method after distillation with a distilling unit (KJELTEC 1026, FOSS, Denmark) and a spectrophotometer (HACH Model DR-2010) in accordance with the guidelines of the 20th Edition of the APHA Standard Methods for the Examination of Water and Wastewater. The TDS concentration was determined using a TDS meter (HI 98312, Hanna Instrument, Woonsocket,

RI, USA) and the chloride concentration was analysed by ion chromatography for both nitrates and nitrites.

2.5.2. Transmission electron microscopy/energy-dispersive X-ray spectroscopy

The fresh and spent NZVI were characterized using a transmission electron microscope (Tecnai G20 TEM, Phillips Electronics Co., Eindhoven, Netherlands). For the TEM analysis, a droplet of diluted NZVI suspension was put on a 300-mesh Cu TEM grid with a carbon film and dried under anaerobic conditions for 24 h. An energy-dispersive X-ray spectroscopy (EDS) analysis was conducted to determine the chemical composition of the NZVI sample.

2.5.3. Particle size and surface area

The particle size was obtained with a particle size analyzer (ELS-8000, Otsuka Electronics Co., Osaka, Japan). The specific surface area was analysed by a Brunauer–Emmett–Teller (BET) surface area analyzer (Sorptomatic 1990 Surface Area Analyzer, Thermo Fisher Scientific Inc., Waltham, MA, USA).

2.5.4. X-ray diffraction analysis

The crystallinity and the iron corrosion products of the nitrate reduction under different electrolyte concentrations were compared by means of an XRD (D/MAX-RB, Rigaku, Tokyo, Japan) analysis with Cu KN radiation. The scan range was 20–90° 2 θ with a scan speed of 1° min⁻¹.

2.5.5. X-ray photoelectron spectroscopy

The change in the chemical binding of the iron species on the surface of the NZVI and the surface chemical composition were obtained through an XPS analysis. Four different samples, prepared under different electrolyte concentrations (0, 0.5, 5, and 12 g/L), were carefully packed on an XPS sampling template under anaerobic conditions to avoid surface oxidation. The XPS analysis was carried out using a MultiLab 2000 (Thermo Electron Co., UK) device with an Al ka X-ray source (1486.6 eV) at a source power of 200 W. Raw spectra were smoothed before being fitted using a Shirley base line and a Gaussian-Lorentzian shape peak. Narrow scanned spectra were used to obtain the chemical state information for iron (Kinetic energy Ek 546 eV) and oxygen (Ek 724 eV).

3. Results and discussion

3.1. NZVI characteristics

The TEM morphologies of the NZVI prepared in this study are shown in Figure 1. The average diameter of the prepared NZVI observed by a laser-scattering particle size analysis was 31.3 nm, while the BET surface area was 18.3 m²/g. The particle size and surface area are comparable

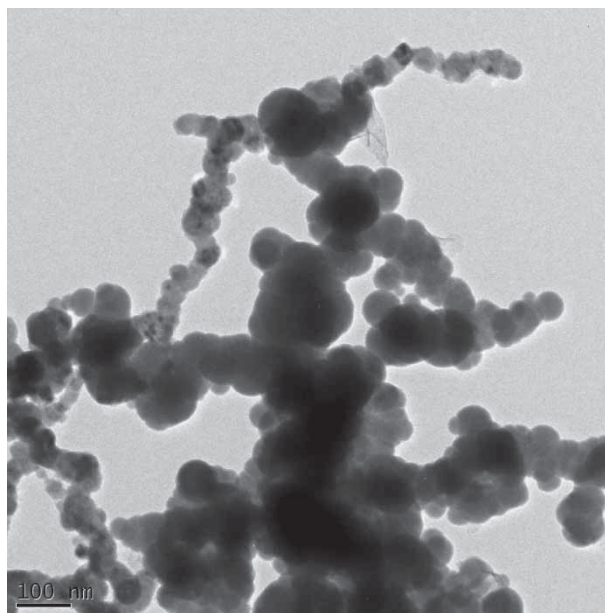


Figure 1. The morphology of the prepared NZVI.

to those in earlier studies. O'Carroll et al. [1] reviewed the NZVI characteristics, finding that the surface area of NZVI can exceed 40 m²/g for stabilized particles and 15–34 m²/g for bare particles, with FeBH having a greater surface area than FeH₂ which is commercially available as reactive nanoscale iron particle (RNIP; Toda Kogyo Corp., Japan).

The NZVI were spherical, with a chain network structure. The spherical shape and chain net morphology are similar to those observed in other studies. The aggregation of NZVI in an aqueous solution without a surfactant is a common behaviour, but it was suggested that the accessibility of reactants to NZVI would not be affected because the total surface area was not affected due to the high porosity of the aggregates.[23]

3.2. Nitrate reduction reactivity by NZVI

3.2.1. Effect of NaCl on NZVI reactivity

The profile of the aqueous nitrate concentration over the reaction time during the nitrate reduction process by NZVI under the reference conditions determined in this study (30 °C, initial pH 7, unbuffered) is presented in Figure S1. The nitrate reduction profile was varied with the amount of NaCl concentration added. Inhibition of the nitrate reduction process was clearly observed when the NaCl dosage exceeded 10 g/L. Without the addition of NaCl, 93.4% of nitrate was reduced after a reaction time of 3 h, while 74.2% of nitrate was reduced with an addition of 10 g/L of NaCl.

The nitrogen mass balance during the reaction is presented in Figure S2. Ammonia was immediately generated as the main reaction product, while a small amount

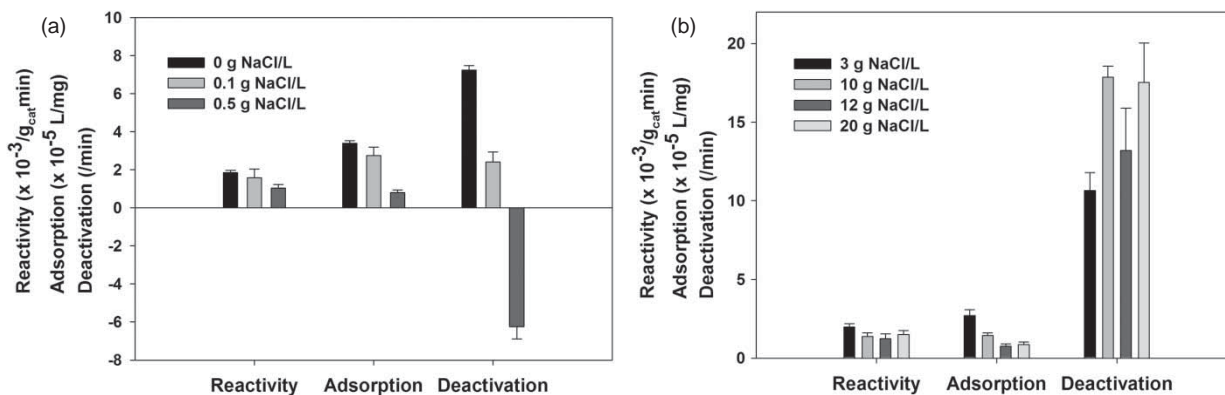


Figure 2. Relationship between the reaction constants and NaCl concentration: (a) low NaCl concentration (1250 mg-Fe/L, 100 mg-NO₃⁻-N/L, 0–0.5 NaCl/L); (b) high NaCl concentration (1250 mg-Fe/L, 100 mg-NO₃⁻-N/L, 3–20 g NaCl/L).

of nitrite was detected. The nitrogen mass balance was held at 74–85.9% (3 h). The nitrogen balance decreased with respect to time due to ammonia stripping under an alkaline pH condition, as described in our previous studies.[18,24] Therefore, the nitrate reduction process can be described as a heterogeneous catalytic reaction which consists of the adsorption of nitrate, the reaction (reduction of nitrate to ammonia), and the desorption of ammonia which is scarcely adsorbed on NZVI.[25] In this study, the LHHW kinetics with inhibition was applied to verify the effect of the NaCl concentration on nitrate reduction by NZVI.

3.2.2. Evaluation of kinetic parameters

As mentioned above, three constants— reactivity, adsorption, and inhibition — were calculated and the data were linearized. Figure 2 (a) presents the reaction constants under a low electrolyte concentration (0–3 g/L). All three constants decreased with the increment of the NaCl concentration. This indicates that the nitrate adsorption and reduction ability of NZVI decreased due to the addition of the electrolyte. On the other hand, the degree of inhibition of the NZVI decreased, which indicates acceleration of nitrate reduction with respect to time.

The low inhibition and acceleration of the nitrate reduction process can be attributed to two factors. First, the addition of chloride ions can enforce the breakdown of the thin film of iron (hydr)oxides on the ZVI surface. Hard Lewis base ions (such as Cl⁻, Br⁻, and I⁻) were reported to be especially aggressive towards passivating oxide layers to form strong complexes with iron centres.[26] As the oxide layers are broken down by these diffusing anions, more of the NZVI surface becomes available for nitrate reduction. Second, chloride can promote localized corrosion on iron with irregular pit shapes, and pitting on the iron surface provides added reactive sites for nitrate reduction.[26]

On the other hand, the opposite result was obtained under a high NaCl concentration (3–20 g/L), as plotted in

Figure 2(b). The rate constant and the adsorption constant decreased, but the inhibition increased with the increment of the NaCl addition. The increased inhibition was the cause of the low nitrate reduction rate under a high NaCl concentration. Therefore, it can be concluded that a high concentration of NaCl can have a negative effect on nitrate reduction by NZVI.

3.3. Inhibition of nitrate reduction by NaCl adsorption on the NZVI surface

3.3.1. Hypothesis

As mentioned in the previous section, it is clear that the added NaCl inhibits nitrate reduction by NZVI. In the research on Pd-based catalytic nitrate reduction, inhibition by sodium chloride is generally accepted. The nitrate reduction activity was completely inhibited at 1000 mg-Cl/L (28.2 mM) due to the preferential sorption of Cl⁻ or the accumulation of Cl⁻ over nitrate in the Helmholtz layer.[27] Moreover, Pintar et al. [28] reported that the catalytic activity levels of Pd-based catalyst were significantly decreased by a NaCl pretreatment (2.5–10 g/L; 42.7–170.9 mM). The repulsion between unconverted nitrate and chloride in the Helmholtz and diffusion layer was enhanced, after which nitrate adsorption was inhibited.

The anion (sulphate) inhibition of NZVI reactivity was reported by Fan et al.[29] They explained that the sulphate ion was adsorbed on the NZVI surface by electric adhesion and that the NZVI reactivity towards azo dye was decreased due to the enhanced repulsion. In addition, the effect of chloride on NZVI reactivity towards perchlorate was reported by Xiong et al.[30] They reported that chloride could enhance the degree of NZVI reactivity, but that the overall reactivity was decreased at a high concentration of NaCl (60 g/L; 1025.6 mM) due to the competition between the chloride ion and perchlorate with regard to sorption. Therefore, it is hypothesized that the added NaCl inhibits nitrate adsorption and that the NZVI reactivity decreases.

3.3.2. NaCl adsorption on the NZVI surface

The chloride concentration in the solution was measured to determine the adsorption on the NZVI surface. The initial and final chloride concentrations (3 h) were measured, and the difference was regarded as the adsorbed fraction by NZVI. 7.7–26.5% of chloride was removed after the reaction. The removed chloride per NZVI dose is presented in Figure S3(a). This shows a linear relationship with the added NaCl concentration. Moreover, the TDS concentration dramatically decreased during the initial period due to the NaCl adsorption on the NZVI surface (Figure S3(b)).

Lastly, the spent NZVI was analysed by an XPS analysis. The XPS analysis was conducted based on the following assumption. If the NaCl was adsorbed on the surface of the NZVI, the adsorbed NaCl would be detected by means of a surface analysis. At a high NaCl concentration, sodium and chloride were detected on the surface of the spent NZVI (Table 1). Therefore, it is clear that the NaCl was adsorbed onto the NZVI surface.

Table 1. Surface element of spent NZVI obtained by XPS.

NaCl (g/L)	Fe	O	Na	Cl
0	17.2	82.8		
0.5	19.2	80.8		
5	18.6	80.1	0.3	1.0
12	16.2	78.7	0.4	4.7

3.3.3. Iron corrosion product and inhibition mechanism with an addition of NaCl

3.3.3.1. Morphology of spent NZVI according to a TEM analysis. In the TEM image, a different morphology was observed under different electrolyte concentrations. For example, spherical iron oxide particles were obtained as a main reaction product of nitrate reduction with no addition of NaCl (Figure 3(a) and 3(b)). On the other hand, two types of iron oxide (iron oxide plates and iron oxide nanoparticles) were observed in the same aggregate

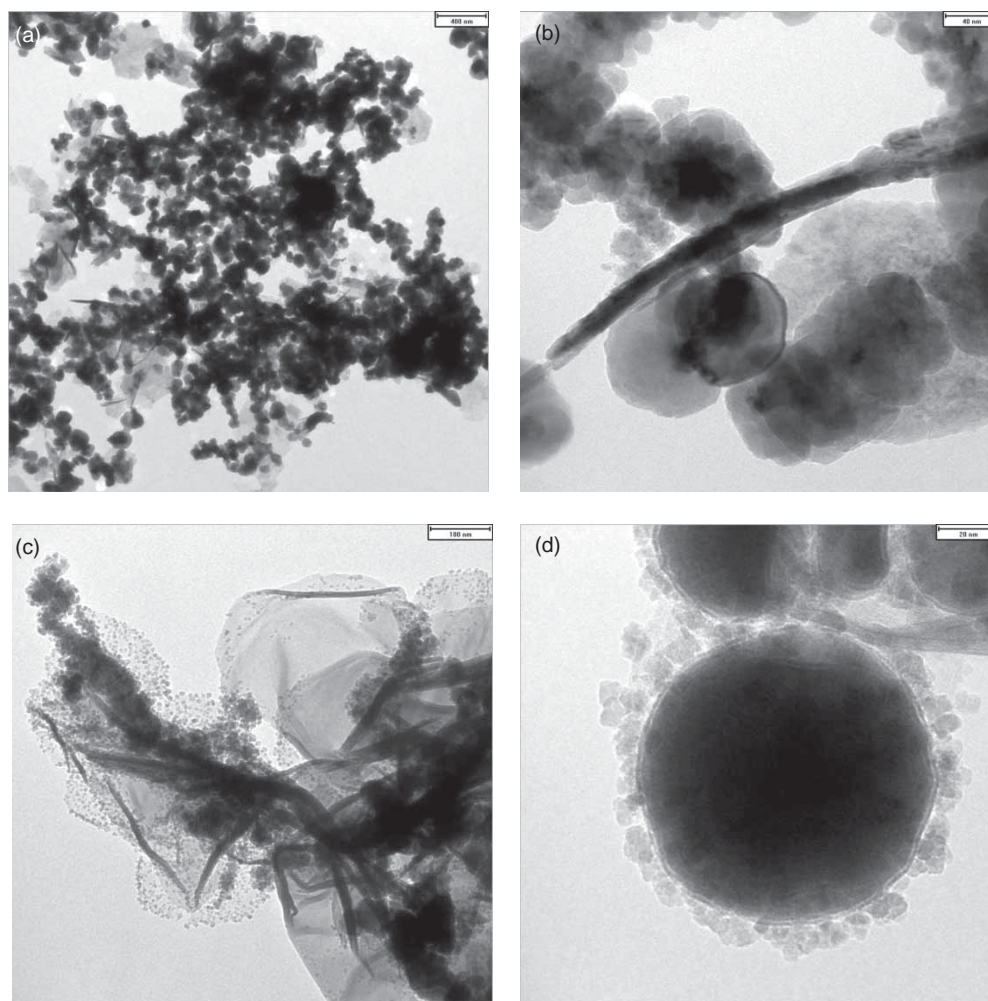


Figure 3. TEM images of spent NZVI: ((a), (b) 1250 mg-Fe/L, 100 mg-NO₃⁻-N/L, 0 g/L of NaCl, (c), (d) 1250 mg-Fe/L, 100 mg-NO₃⁻-N/L 12 g/L of NaCl).

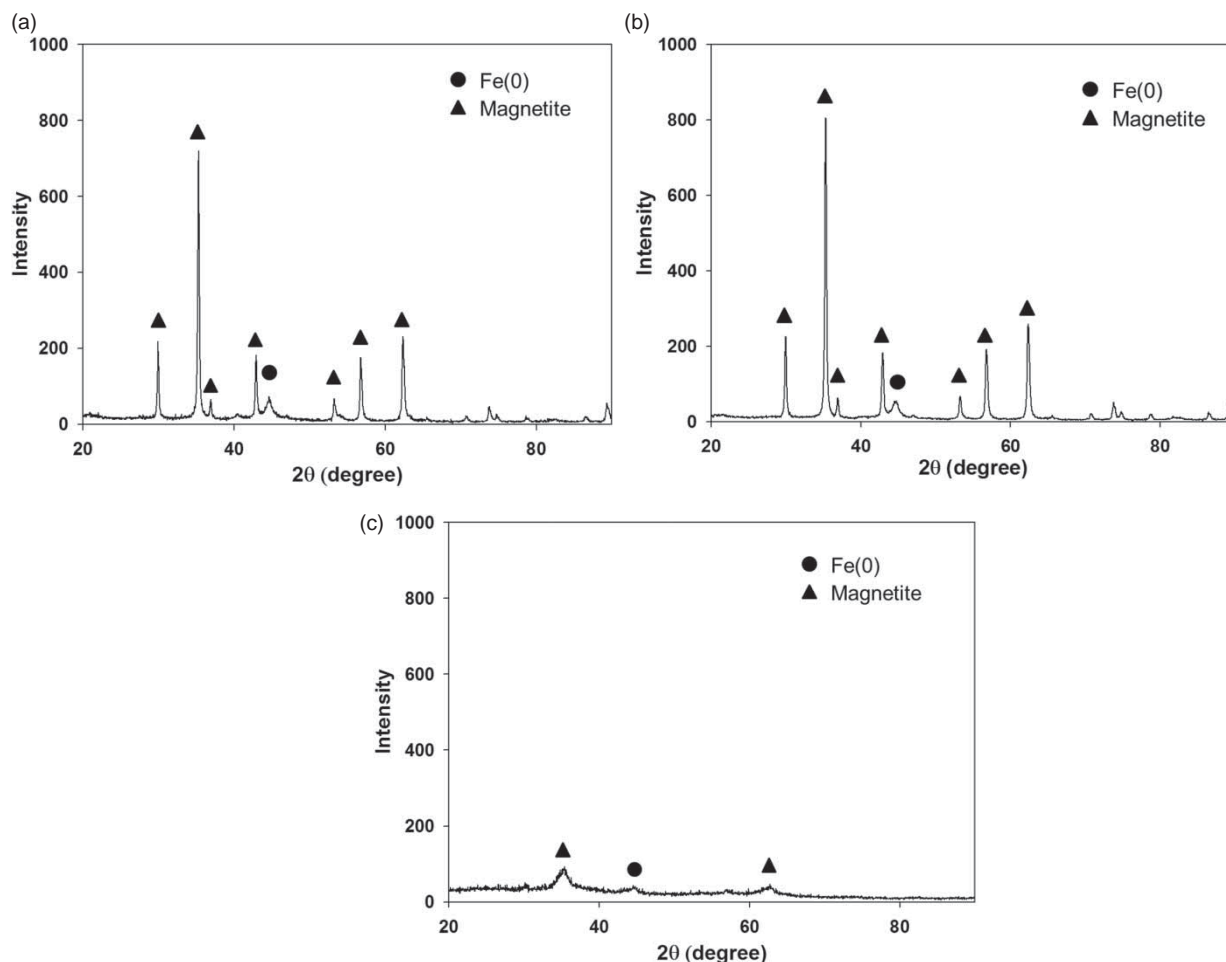


Figure 4. XRD peaks of the spent NZVI under different NaCl concentrations: (a) 0 g/L, (b) 0.5 g/L, and (c) 12 g/L.

after an addition of 12 g/L NaCl (Figure 3(c)). Moreover, core-shell structured NZVI remained in the sample (Figure 3(d)), and tiny surface particles were observed. The core-shell structure was verified by an EDS analysis. Figure S4 clearly shows that the shell consists of iron oxide, while the core mainly consists of zero-valent iron. This finding indicates that the NZVI was not completely oxidized under a high NaCl concentration.

Ryu et al. [31] reported that both iron oxide morphologies (iron oxide plates and iron oxide nanoparticles) could be obtained as the reaction product of nitrate reduction by NZVI. In particular, iron oxide nanoparticles were produced from the nitrate reduction while an iron oxide plate was produced by oxidation when oxygen was exposed to NZVI during the synthesis process or via NZVI oxidation by water. Therefore, the high fraction of the iron oxide plates and the low fraction of iron oxide nanoparticles in the spent NZVI sample at 12 g/L NaCl were in agreement with the low nitrate reduction reactivity by NZVI.

Ryu et al. [31] also suggested that not all NZVI particles participate in the reaction simultaneously but instead react as particles or branch units until their reduction

capacity is exhausted, with other particles or branches of NZVI remain in their original states. This is also in agreement with the existence of unreacted NZVI particles (core-shell structured NZVI) in the spent NZVI sample at 12 g/L NaCl. Therefore, the reaction product was clearly changed by the addition of NaCl.

3.3.3.2. Crystallinity and end products determined by XRD analysis. The crystallinity and end products were determined by an XRD analysis. Figure 4 shows the XRD patterns with different amounts of NaCl added (0, 0.5, 12 g/L). When NaCl was not added, the XRD pattern clearly shows that the end product is magnetite. The same XRD pattern was observed at a low concentration of NaCl. However, very broad peaks with a low intensity were observed under high NaCl concentrations. This indicates that the end product is poorly crystalline with a high NaCl concentration. The end products may be amorphous iron hydroxide, which is an intermediate product between NZVI and magnetite.

As mentioned above, pitting corrosion occurred when a chloride solution was used and led to a permeable shell

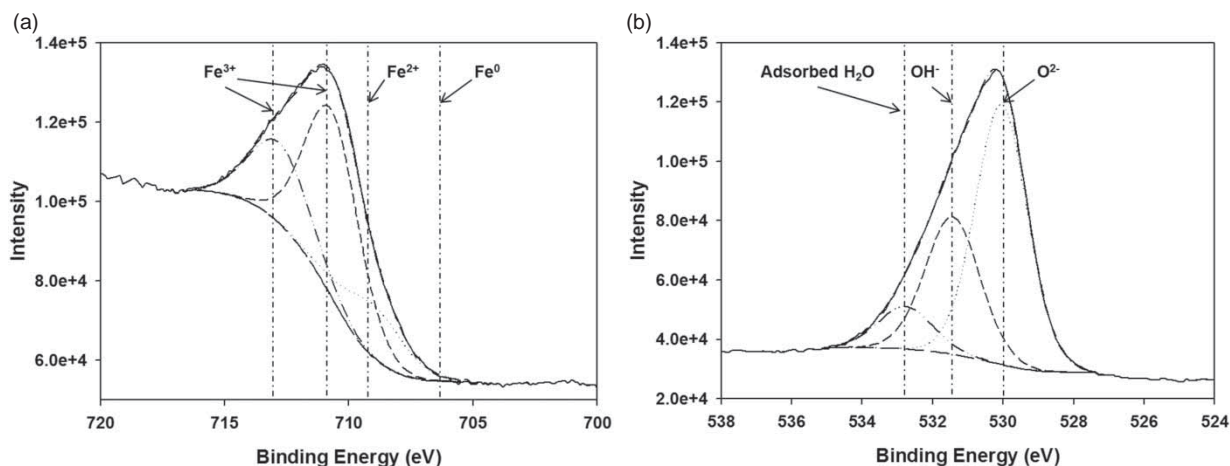


Figure 5. XPS scan of the spent NZVI (0 g/L): (a) Fe 2p scan, (b) O 1s scan.

Table 2. Chemical compositions on the surface of the spent NZVI.

		0 g/L	0.5 g/L	5 g/L	12 g/L
Fe	Fe ⁰	0.3	0.2	1.1	0
	Fe(II)	17.3	17.6	12.7	8.2
	Fe(III)	82.4	82.2	86.2	91.8
O	O ²⁻	57.9	68.5	56.4	47.9
	OH ⁻	32.1	21.5	33.7	42.4
	Absorbed H ₂ O	10.0	10.0	9.9	9.7

structure that consists of iron hydroxide.[30] After the redox reaction was finished, all of the ZVI was converted to magnetite, which was the final end product of the reaction. The reason for the generation of an intermediate product in such a case would be the inhibition of nitrate adsorption by electrolyte adsorption. This can explain the decrease in the reactivity at the high electrolyte concentration.

3.3.3.3. Surface chemical composition by XPS analysis.

The surface chemical composition was obtained by XPS to verify the end products and the inhibition mechanism. Figure 5 provides narrow scans of Fe (2p_{3/2}) and O (1s) on the surfaces of the controls (no NaCl) with their binding energies. The narrow region spectra for Fe(2p_{3/2}) are composed of four identical peaks at 706.42, 709.32–709.59, 711–711.18, and 712.52–713.33 eV (Figure 5 (a)). It has been reported that the binding energies for Fe(0), Fe(II)-O, and Fe(III)-O were 706.4, 709–709.5, and 711–714 eV, respectively.[32] The O (1s) spectrum presented in Figure 5 (b) is broad and is best fitted with three components at 529.5, 531.3 and 532.5 eV. These correspond to oxide oxygen, hydroxyl groups, and adsorbed water, respectively.[33] Table 2 shows the surface composition of the Fe species on the different solid surfaces.

In the control sample (no NaCl), 82.4% of the iron was found to exist in the form of Fe(III)-O, and 17.3% existed

as Fe(II)-O. Moreover, the bound oxygen was found to consist of 57.9% in the oxide form, 32.1% in the hydroxide form, and 10% water.

After the addition of 0.5 g/L NaCl, the chemical state of iron was fairly similar to that of the control. However, the chemical state of oxygen was found to vary. The oxide form of oxygen increased to 68.5%. This indicates that the fraction of iron oxide increased in the end product more than it did in the control. This result is coincident with the XRD results, which show a higher corresponding peak intensity level.

On the other hand, the fraction of Fe(III)-O was significantly increased to 91.8% after an addition of 12 g/L NaCl. This indicates that the surface was more oxidized. For oxygen, the hydroxide portion was increased to 42.4%.

As a result of iron oxidation and nitrate reduction, dissolution of the metal occurs at the anodic sites, releasing ions which may then react to form insoluble corrosion products. This film of (oxy)hydroxides which develops on NZVI evolves into a complex layered structure as a result of oxidation, recrystallization, and precipitation.[34] The formation of this passivating film of iron oxides appears to be responsible for the decreased rate of the NZVI-mediated reaction.[35]

However, the formation of the passivation oxide/hydroxide film was inhibited by chloride ions. The HCl produced by metal hydrolysis with chloride reacts with the metal to produce ferrous chloride and hydrogen, or ferric chloride and water. Hydrolysis of the metal chloride forms Fe(OH)₂ (which is non-passivating).[14]

3.3.3.4. Inhibition mechanism. As a result of the characterization of the spent NZVI, the inhibition mechanism of NZVI on nitrate reduction by a high concentration of NaCl could be achieved. The NZVI was completely oxidized to iron oxide regardless of the existence of NaCl at a low concentration (0.1–0.5 g/L). The iron oxide nanoparticles, the

magnetite peak, and the high fraction of the Fe(II)-O oxide form of oxygen were assessed by TEM, XRD, and XPS, respectively.

On the other hand, NZVI oxidation was inhibited by NaCl adsorption with a high concentration of NaCl (> 3 g/L). The iron oxide plates and unoxidized NZVI were obtained according to a TEM analysis, and poorly crystallized iron oxide was obtained according to an XRD analysis. Although the permeable iron (oxy)hydroxide was obtained on the surface of spent NZVI by means of chloride attack according to an XPS analysis, the Fe(0) in the core was not completely oxidized. Moreover, the iron (oxy)hydroxide is the main component of the shell structure in core-shell NZVI,[36] and it is an intermediate product between NZVI and magnetite. Therefore, the inhibition effect of a high NaCl concentration is due to the competitive adsorption of anions on the NZVI surface, as in Pd-based catalytic nitrate reduction.[27] Because the nitrate reduction by NZVI was determined to be a heterogeneous catalytic reaction, which could be interpreted by the LHHW equation, the adsorption of nitrate is a prerequisite for the entire reaction. However, the accumulation of Cl⁻ on the surface or the Helmholtz layer of NZVI had a negative effect on the adsorption of nitrate by electric repulsion.[28–30] This may have caused the decreased reactivity under a high NaCl concentration.

4. Conclusion

In this study, different effects depending on the electrolyte concentration on nitrate reduction and on the characteristics of NZVI were investigated. At a low concentration (0–3 g/L), the reactivity was decreased during the initial reaction period. However, the reactivity was increased after a certain time as the corrosion process was accelerated. On the other hand, the reactivity at a high electrolyte concentration (3–20 g/L) was significantly decreased due to the inhibition effect of the electrolyte.

The chloride and TDS concentration decreased after reacting for 3 h. Moreover, sodium chloride was obtained by an XPS analysis. This clearly shows that the electrolyte was adsorbed onto the NZVI surface and that the active sites on the NZVI surface were blocked by the adsorbate.

The characteristics of NZVI varied significantly after the reaction under different electrolyte concentrations. The NZVI was completely oxidized to iron oxide regardless of whether NaCl was absent or present at a low concentration (0.1–0.5 g/L). On the other hand, the NZVI oxidation was inhibited by electrolyte adsorption with a high concentration of NaCl (> 3 g/L). An iron oxide plate, unoxidized NZVI, and poorly crystallized iron oxide were obtained. Iron (oxy)hydroxide was also obtained on the surface of the spent NZVI according to an XPS analysis. It is the main component of the shell structure in core-shell NZVI. This clearly shows that iron oxidation was inhibited by NaCl adsorption.

Disclosure statement

No potential conflict of interest was reported by the author(s).

Supplemental data

Supplemental data for this article can be accessed at <http://dx.doi.org/10.1080/09593330.2014.982723>.

References

- [1] O'Carroll D, Sleep B, Krol M, Boparai H, Kocur C. Nanoscale zero-valent iron and bimetallic particles for contaminated site remediation. *Adv Water Resour.* 2013;51:104–122.
- [2] Crane RA, Scott TB. Nanoscale zero-valent iron: future prospects for an emerging water treatment technology. *J Hazard Mater.* 2012;211–212:112–125.
- [3] Wang CB, Zhang WX. Synthesizing nanoscale iron particles for rapid and complete dechlorination of TCE and PCBs. *Environ Sci Technol.* 1997;31:2154–2156.
- [4] Klimkova S, Cernik M, Lacinova L, Filip J, Jancik D, Zboril R. Zero-valent iron nanoparticles in treatment of acid mine water from in situ uranium leaching. *Chemosphere.* 2011;82:1178–1184.
- [5] Crane RA, Dickinson M, Popescu IC, Scott TB. Magnetite and zero-valent iron nanoparticles for the remediation of uranium contaminated environmental water. *Water Res.* 2011;45:2931–2942.
- [6] Mauguin G, Corsin P. Concentrate and other waste disposals from SWRO plants: characterization and reduction of their environmental impact. *Desalination.* 2005;182:355–364.
- [7] Mickley M. Treatment of concentrate: final report. U.S. Bureau of Reclamation: Denver; 2007.
- [8] Huang RM, He JY, Zhao J, Luo Q, Huang CM. Fenton-biological treatment of reverse osmosis membrane concentrate from a metal plating wastewater recycle system. *Environ Technol.* 2011;32:515–522.
- [9] Westerhoff P, Moon H, Minakata D, Crittenden J. Oxidation of organics in retentates from reverse osmosis wastewater reuse facilities. *Water Res.* 2009;43:3992–3998.
- [10] Zhou T, Lim TT, Chin SS, Fane AG. Treatment of organics in reverse osmosis concentrate from a municipal wastewater reclamation plant: feasibility test of advanced oxidation processes with/without pretreatment. *Chem Eng J.* 2010;166:932–939.
- [11] Dialynas E, Mantzavinos D, Diamadopoulos E. Advanced treatment of the reverse osmosis concentrate produced during reclamation of municipal wastewater. *Water Res.* 2008;42:4603–4608.
- [12] Van Hege K, Verhaege M, Verstraete W. Electro-oxidative abatement of low-salinity reverse osmosis membrane concentrates. *Water Res.* 2004;38:1550–1558.
- [13] Ghanch A, Tuqan A, Assi HA. Antibiotic removal from water: elimination of amoxicillin and ampicillin by microscale and nanoscale iron particles. *Environ Pollut.* 2009;157:1626–1635.
- [14] Kim JS, Shea PJ, Yang JE, Kim JE. Halide salts accelerate degradation of high explosives by zero-valent iron. *Environ Pollut.* 2007;147:634–641.
- [15] Comba S, Sethi R. Stabilization of highly concentrated suspensions of iron nanoparticles using shear-thinning gels of xanthan gum. *Water Res.* 2009;43:3717–3726.
- [16] Choe SH, Chang YY, Hwang KY, Khim J. Kinetics of reductive denitrification by nanoscale zero-valent iron. *Chemosphere.* 2000;41:1307–1311.

- [17] Park H, Park YM, Oh SK, You KM, Lee SH. Enhanced reduction of nitrate by supported nanoscale zero-valent iron prepared in ethanol-water solution. *Environ Technol.* 2009;30:261–267.
- [18] Hwang YH, Kim DG, Shin HS. Mechanism study of nitrate reduction by nano zero-valent iron. *J Hazard Mater.* 2011;185:1513–1521.
- [19] Kumar KV, Porkodi K, Rocha F. Langmuir-Hinshelwood kinetics: a theoretical study. *Catal Commun.* 2008;9:82–84.
- [20] Katsenovich YP, Miralles-Wilhelm FR. Evaluation of nanoscale zerovalent iron particles for trichloroethene degradation in clayey soils. *Sci Total Environ.* 2009;407:4986–4993.
- [21] Sarathy V, Tratnyek PG, Nurmi JT, Baer DR, Amonette JE, Chun CL, Penn RL, Reardon EJ. Aging of iron nanoparticles in aqueous solution: effects on structure and reactivity. *J Phys Chem C.* 2008;112:2286–2293.
- [22] Kim DG, Hwang YH, Shin HS, Ko SO. Deactivation of nanoscale zero-valent iron by humic acid and by retention in water. *Environ Technol.* 2013;34:1625–1635.
- [23] Yang GCC, Lee HL. Chemical reduction of nitrate by nano-sized iron: kinetics and pathways. *Water Res.* 2005;39:884–894.
- [24] Hwang YH, Kim DG, Ahn YT, Moon CM, Shin HS. Fate of nitrogen species in nitrate reduction by nanoscale zero-valent iron and characterization of the reaction kinetics. *Water Sci Technol.* 2010;61:705–712.
- [25] Chen YM, Li CW, Chen SS. Fluidized zero-valent iron bed reactor for nitrate removal. *Chemosphere.* 2005;59:753–759.
- [26] Gotpagar J, Lyuksyutov S, Cohn R, Grulke E, Bhat-tacharyya D. Reductive dehalogenation of trichloroethylene with zero-valent iron: surface profiling microscopy and rate enhancement studies. *Langmuir.* 1999;15:8412–8420.
- [27] Chaplin BP, Roundy E, Guy KA, Shapley JR, Werth CJ. Effects of natural water ions and humic acid on catalytic nitrate reduction kinetics using an alumina supported Pd – Cu catalyst. *Environ Sci Technol.* 2006;40:3075–3081.
- [28] Pintar A, Batista J, Muševič I. Palladium-copper and palladium-tin catalysts in the liquid phase nitrate hydro-genation in a batch-recycle reactor. *Appl Catal B-Environ.* 2004;52:49–60.
- [29] Fan J, Guo Y, Wang J, Fan M. Rapid decolorization of azo dye methyl orange in aqueous solution by nanoscale zero-valent iron particles. *J Hazard Mater.* 2009;166:904–910.
- [30] Xiong Z, Zhao D, Pan G. Rapid and complete destruction of perchlorate in water and ion-exchange brine using stabilized zero-valent iron nanoparticles. *Water Res.* 2007;41:3497–3505.
- [31] Ryu A, Jeong SW, Jang A, Choi H. Reduction of highly concentrated nitrate using nanoscale zero-valent iron: Effects of aggregation and catalyst on reactivity. *Appl Catal B-Environ.* 2011;105:128–135.
- [32] Bae S, Lee W. Inhibition of nZVI reactivity by magnetite during the reductive degradation of 1,1,1-TCA in nZVI/magnetite suspension. *Appl Catal B-Environ.* 2010;96:10–17.
- [33] Mullet M, Boursiquot S, Abdelmoula M, Génin JM, Ehrhardt JJ. Surface chemistry and structural properties of mackinawite prepared by reaction of sulfide ions with metallic iron. *Geochim Cosmochim Ac.* 2002;66:829–836.
- [34] Agrawal A, Ferguson WJ, Gardner BO, Christ JA, Ferguson WJ, Bandstra JZ, Tratnyek PG. Effects of carbonate species on the kinetics of dechlorination of 1,1,1-Trichloroethane by zero-valent iron. *Environ Sci Technol.* 2002;36:4326–4333.
- [35] Joo SH, Feitz AJ, Waite TD. Oxidative degradation of the carbothioate herbicide, molinate, using nanoscale zero-valent iron. *Environ Sci Technol.* 2004;38:2242–2247.
- [36] Theron J, Walker JA, Cloete TE. Nanotechnology and water treatment: applications and emerging opportunities. *Crit Rev Microbiol.* 2008;34:43–69.